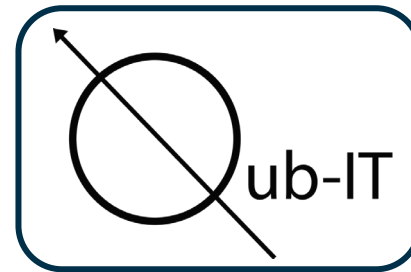


# Quantum Sensing with superconducting qubits for Fundamental Physics

**Roberto Moretti**

roberto.moretti@mib.infn.it

On behalf of the **Qub-IT** collaboration



16<sup>th</sup> Workshop on Low Temperature Electronics



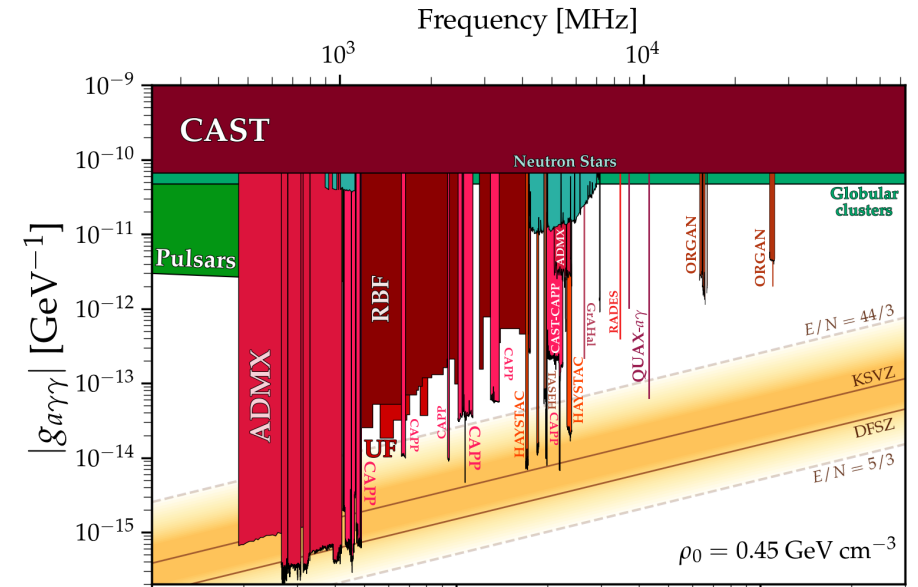
# Low-mass Dark Matter

## Axion

- Would solve the strong CP problem.

$$\mathcal{L} = -\frac{1}{4} F^{\mu\nu} F_{\mu\nu} + \theta \frac{g^2}{32\pi^2} F^{\mu\nu} \tilde{F}_{\mu\nu} + \bar{\psi}(i\gamma^\mu D_\mu - me^{i\theta'\gamma_5})\psi$$

- Single-photon conversion is expected (inverse Primakoff).
- Strong magnetic field required to boost conversion.



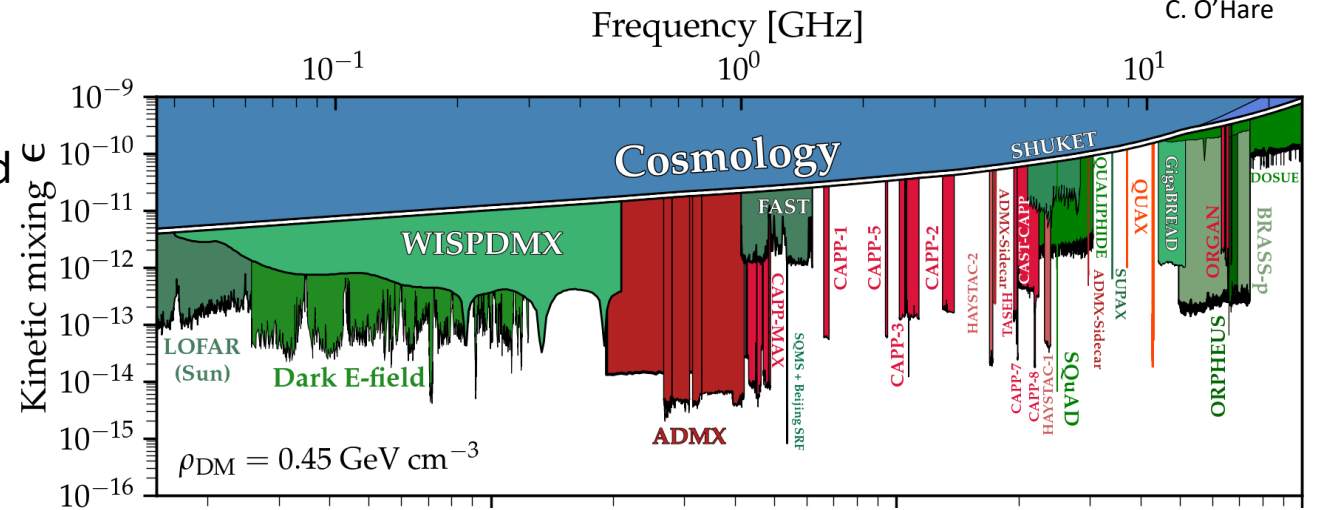
10.5281/zenodo.3932430

C. O'Hare

## Dark Photon

- Gauge U(1) symmetry not included in the Standard Model
- Kinetic mixing with the EM field

$$\mathcal{L} = -\frac{1}{4} F'^{\mu\nu} F'_{\mu\nu} + \frac{1}{2} m_{A'}^2 A'^\mu A'_\mu + \epsilon e A'^\mu J_\mu^{EM}$$



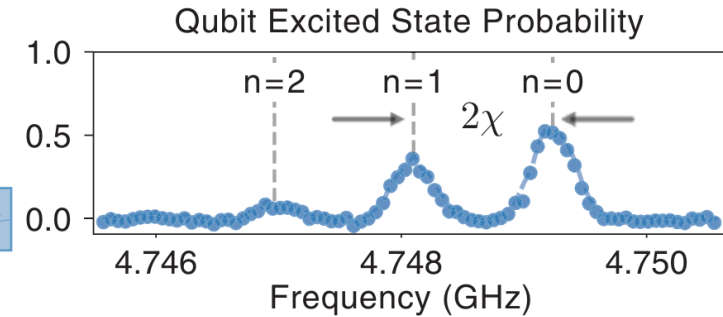
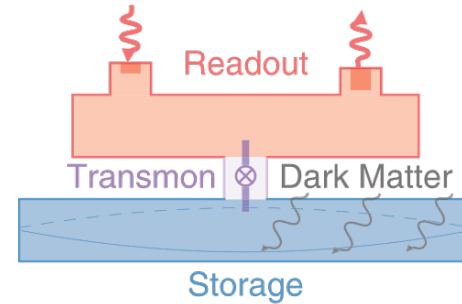
# Transmon as QND detection platforms

## Quantum Non-Demolition

The interaction between Dark Matter candidates and EM field leads to a photon deposited in a storage cavity.

$$\hat{\mathcal{H}} = \omega_r a^\dagger a + \frac{1}{2} (\omega_q + 2\chi a^\dagger a) \hat{\sigma}_z$$

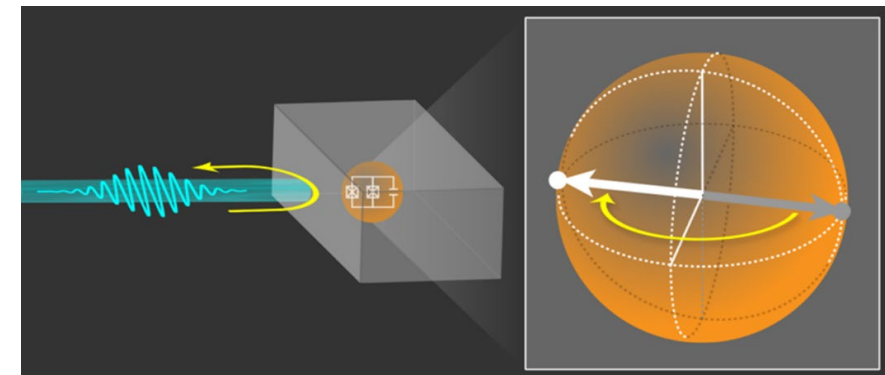
Photon-dependent precession term



[10.1103/PhysRevLett.126.141302](https://doi.org/10.1103/PhysRevLett.126.141302)  
A. V. Dixit et al. (2021)

## Itinerant photon detection

- Transmon coupled to a cavity far from the magnetic field in  $|+\rangle$  state.
- The microwave photon produced in the magnetic field region travels towards the cavity.
- Photon-qubit interaction acquires a  $\pi$  phase shift.



[10.1038/s41567-018-0066-3](https://doi.org/10.1038/s41567-018-0066-3)  
S. Kono et al. (2018)

[10.1103/PhysRevX.8.021003](https://doi.org/10.1103/PhysRevX.8.021003)  
J. C. Besse et al. (2018)

Image credit: APS/Alan Stonebraker

# Transmon as direct detection platforms

We can detect hidden AC field through the excitation of Transmons when on resonance with the Dark Photon's mass.

Dark photon field:  $\vec{X} = X\vec{\eta} \cos(m_X t)$   
 Total field on qubit:  $\vec{E}_{eff} = \vec{E}_{EM} + \vec{E}_X = \vec{E}_{EM} - \epsilon\vec{X}$

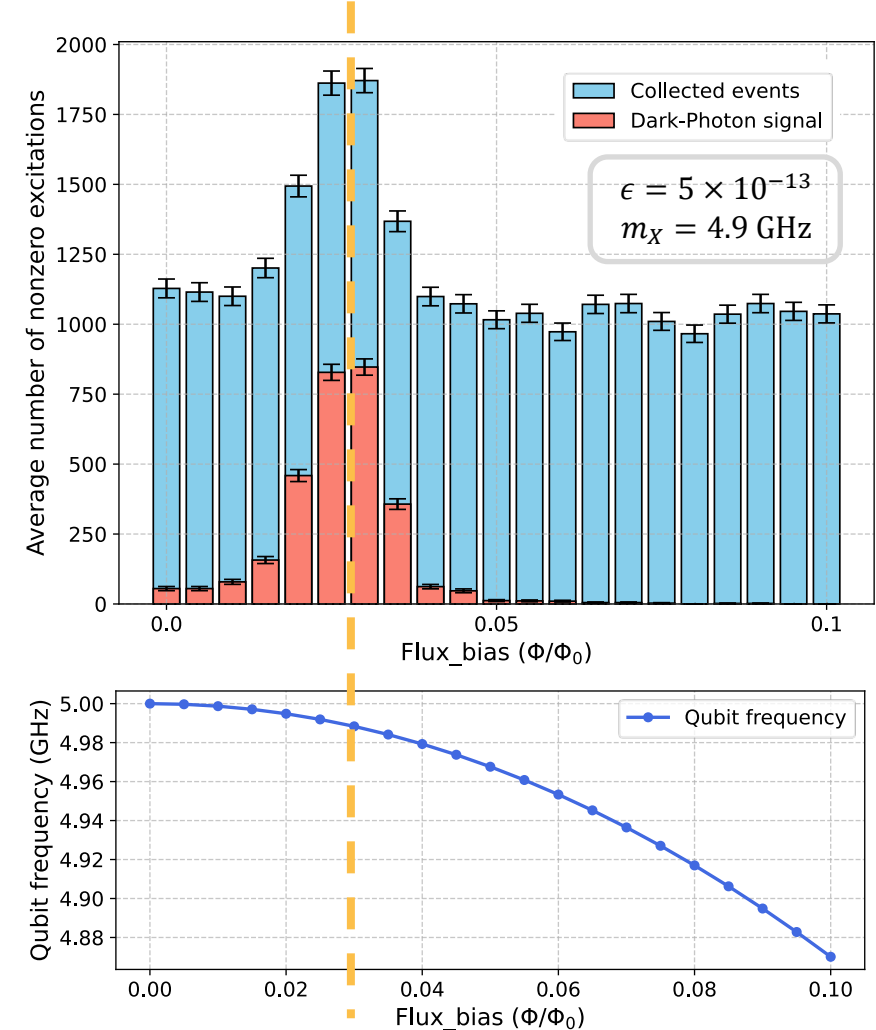
DM exerts a slow Rabi oscillation on a qubit state:

$$p_{ge}(\tau) \approx 0.04 \times \left(\frac{\epsilon}{10^{-11}}\right)^2 \left(\frac{f}{1 \text{ GHz}}\right) \left(\frac{\tau}{100 \mu\text{s}}\right)^2 \left(\frac{C}{0.1 \text{ pF}}\right) \left(\frac{d}{100 \mu\text{m}}\right)^2 \left(\frac{\rho_{DM}}{0.45 \text{ GeV/cm}^3}\right)$$

Resonant frequency  $\uparrow$   $f$   $\uparrow$  Shunt capacitance  $\uparrow$   $C$   $\uparrow$  DM local density  $\uparrow$   $\rho_{DM}$   
 Kinetic mixing  $\leftarrow$   $\epsilon$   $\leftarrow$  Evolution time  $\leftarrow$   $\tau$   $\leftarrow$  Distance between plates  $\leftarrow$   $d$

10.1103/PhysRevLett.131.211001  
S. Chen et al. (2023)

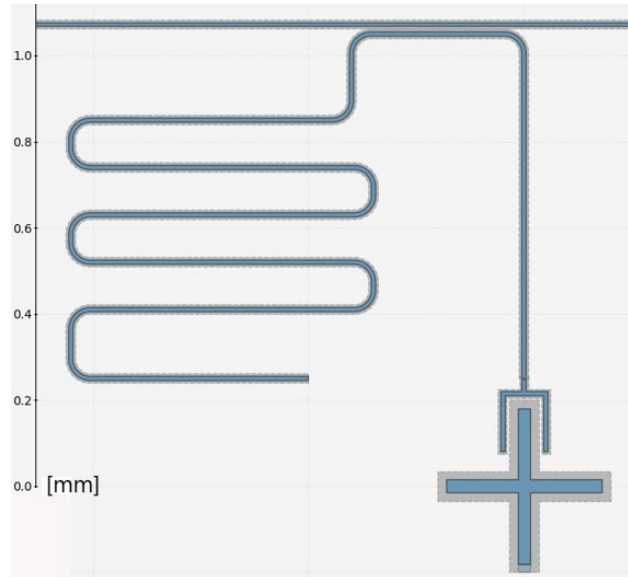
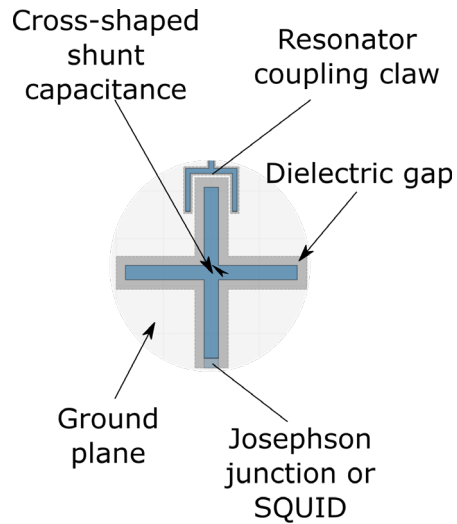
MC simulation



# Test chip design

## QND – v0

- Design software: Qiskit Metal (**IBM**).
- Grounded (X-mon) qubits.

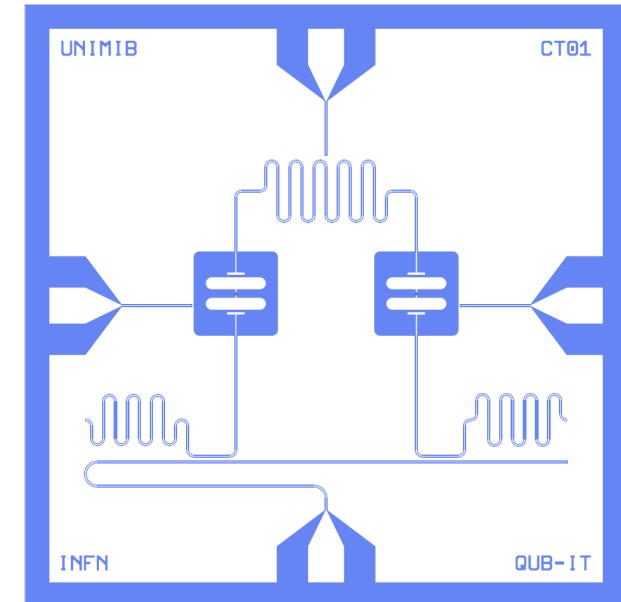
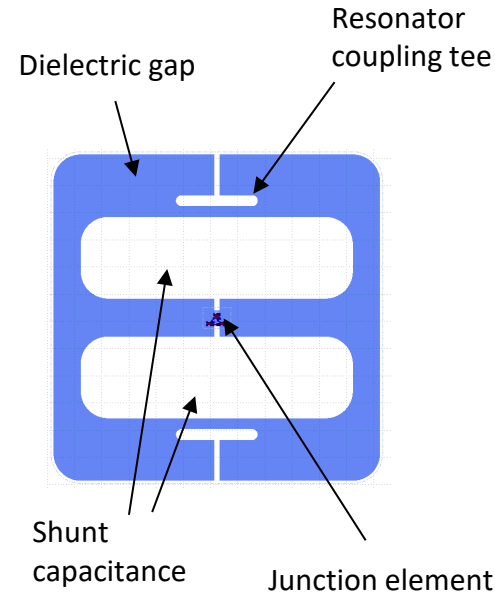


[10.1109/TASC.2024.3350582](https://arxiv.org/abs/10.1109/TASC.2024.3350582)  
R. Moretti et al. (2024)

- High dispersive shift  $\chi$  needed.
- Already **fabricated** and **tested**.

## QND – v1

- Design software: KQCCircuits (**IQM**).
- Floating (Double-pads) qubits.

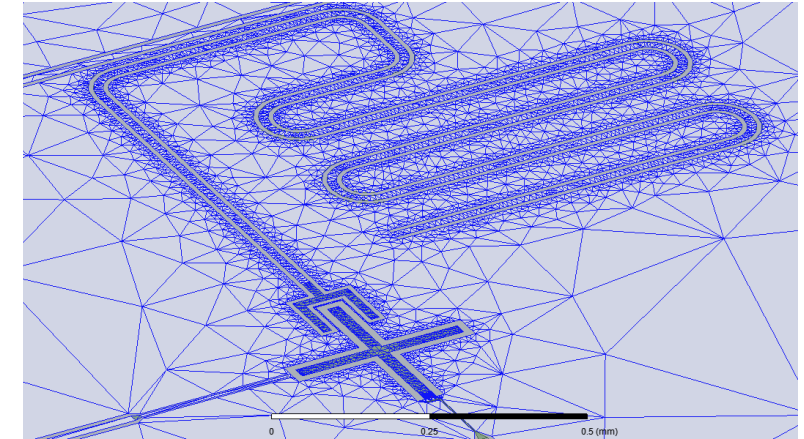
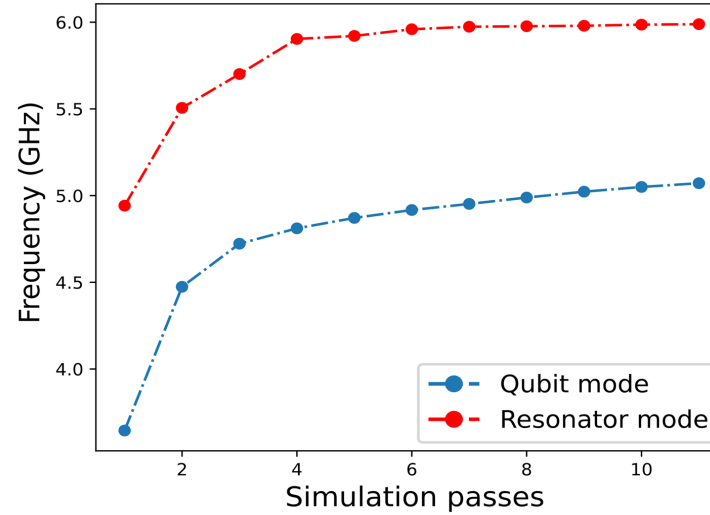


- High dispersive shift for both qubits  $\chi_1, \chi_2$ , with  $\chi_1 \approx \chi_2$
- Further dark count suppression.
- Allows experiments on entangled-states.
- **To be optimized.**

# Energy Participation Ratio

The EPR analysis computes the system eigenmodes  $|\psi_m\rangle$  with  $m \in \{\text{qubit, cavity}\}$  and computes the energy participation ratio:

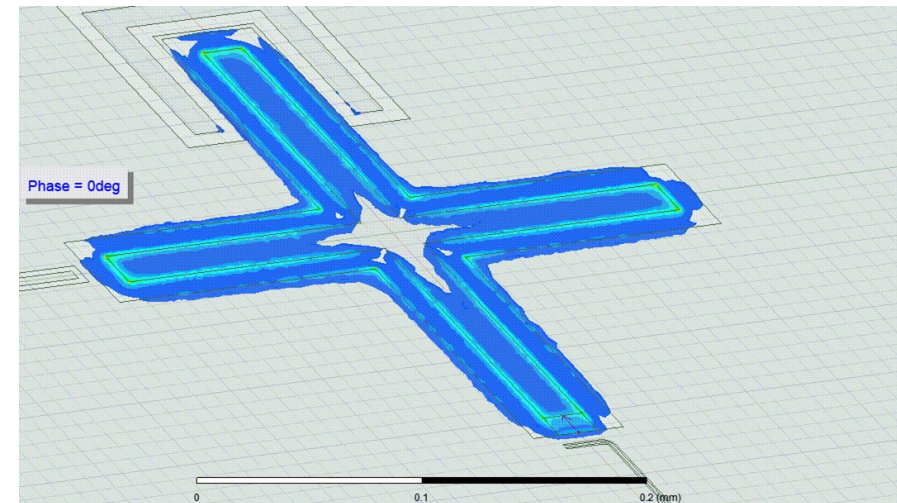
$$p_m = \frac{\text{Inductive energy in JJ}}{\text{Inductive energy stored in mode}} = \frac{\langle \psi_m | \frac{1}{2} E_J \hat{\Phi}_J | \psi_m \rangle}{\langle \psi_m | \frac{1}{2} \hat{H}_{lin} | \psi_m \rangle}$$



Where  $\hat{H}_{lin} = \hbar\omega_c \hat{a}_c^\dagger \hat{a}_c + \hbar\omega_q \hat{a}_q^\dagger \hat{a}_q$

**Kerr matrix**  $\chi_{mm'} = \frac{\hbar\omega_m \omega_{m'}}{4E_J} p_m p_{m'}$

10.1038/s41534-021-00461-8  
Z. K. Mineev et al. (2021)

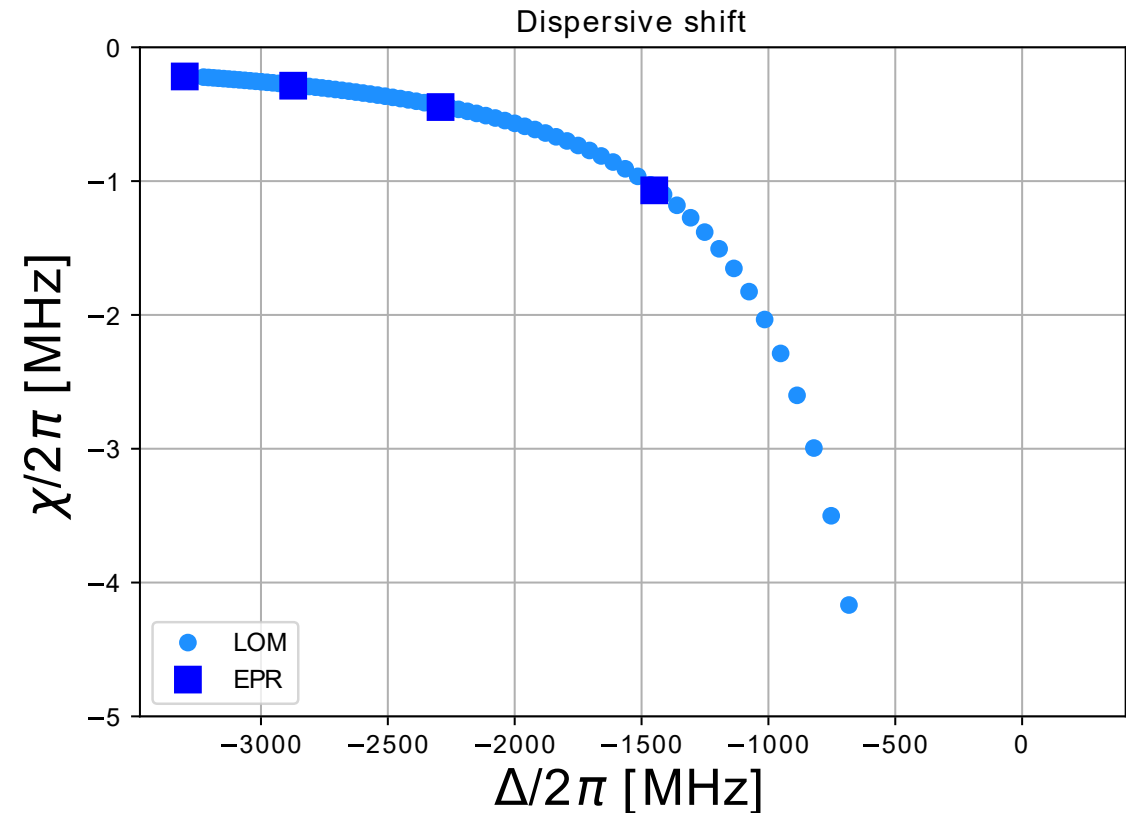


# EPR and Lumped Oscillator Model

- EPR: Energy Participation Ratio.
- LOM: Lumped Oscillator Model (analytical extraction).

	Target	LOM	EPR
JJ inductance $L_J$ [nH]	10	10	10
Transmon regime $E_J/E_c$	>50	78.61	79.96
Anharmonicity $\alpha/2\pi$ [MHz]	202	230.62	216.44
Dispersive shift $\chi/2\pi$ [MHz]	0.30	0.31	0.35
Qubit frequency $\omega_q/2\pi$ [MHz]	5000	4995.79	4893.84
Cavity frequency $\omega_c/2\pi$	7400	7481.04	7435.44
Qubit-cavity coupling $C_g$ [fF]	4	3.93	-

$$T_{1 \text{ Purcell}} \approx 51 \mu\text{s for } Q_c \approx 4 \times 10^3$$

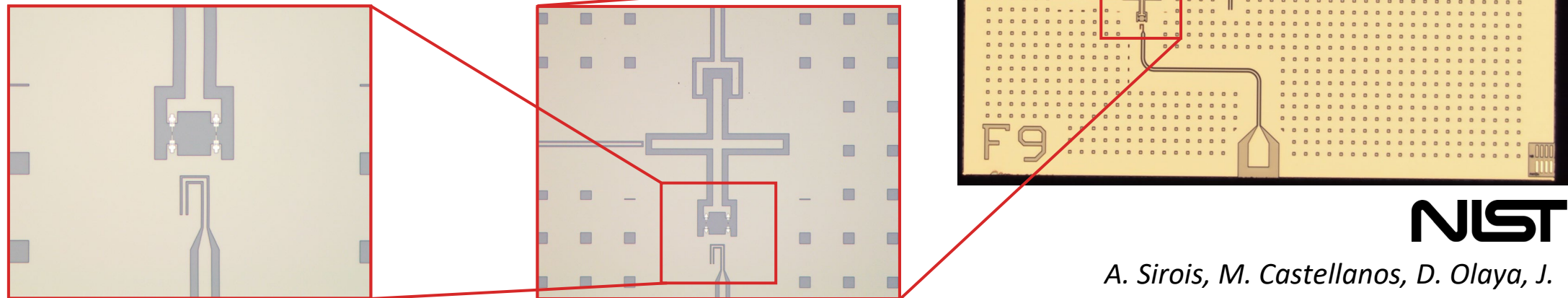


# First chip fabrication

A demonstrative two-qubit chip has been fabricated at **NIST**

- One fixed-frequency, resonator driven transmon
- One tunable-frequency, dedicated drive-line.

**Aim:** verify the correspondence between design and measured parameters.



*A. Sirois, M. Castellanos, D. Olaya, J. Bieseker, P. Hopkins, S. Benz.*

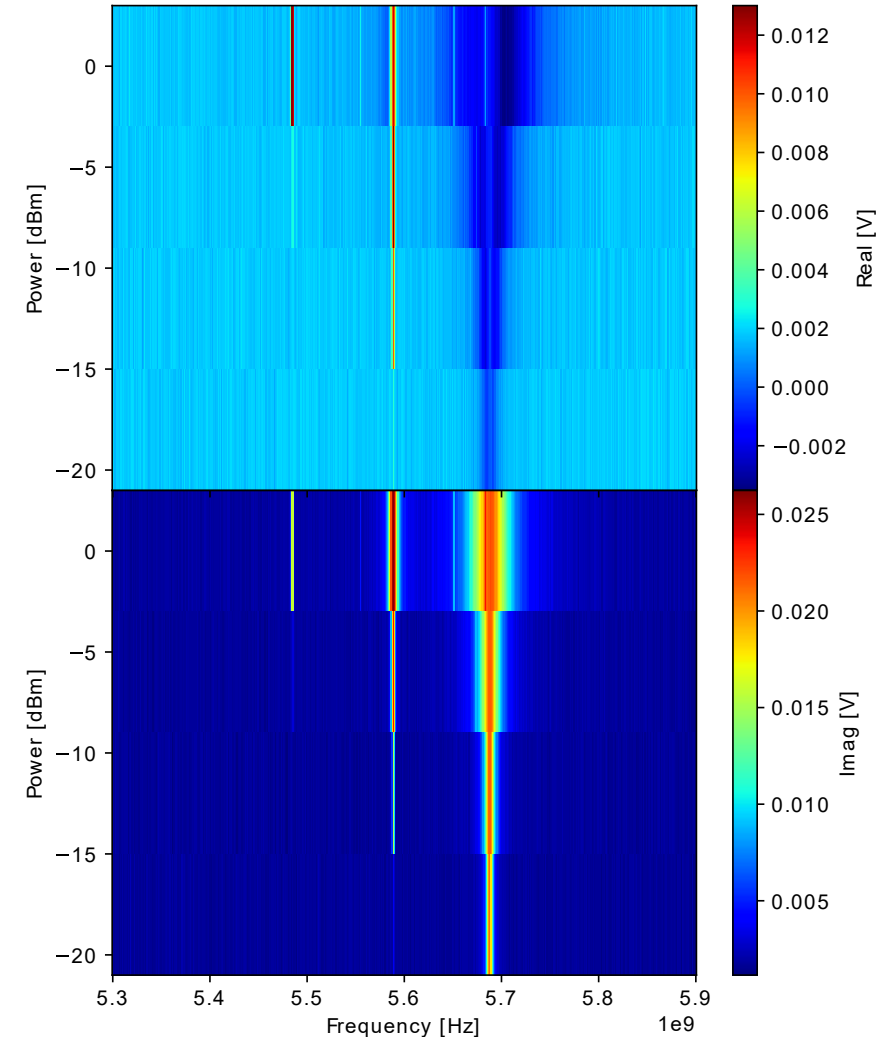
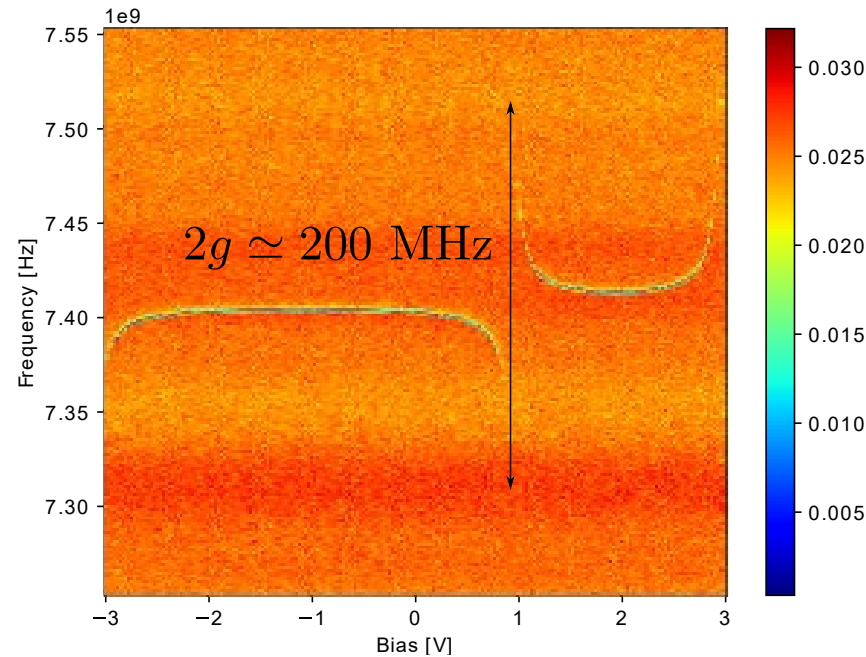


# Agreement with simulations

Standard characterization carried out at NIST.  
Good agreement between experiments and simulations.

Fixed qubit	Measured	LOM
$\omega_{0 \rightarrow 1} / 2\pi$ [GHz]	5.689	5.682
$\frac{1}{2} \omega_{0 \rightarrow 2} / 2\pi$ [GHz]	5.589	5.579
$\omega_{1 \rightarrow 2} / 2\pi$ [GHz]	5.485	5.476
$\alpha / 2\pi$ [MHz]	204	206
$L_J$ [nH]	7.641	7.2

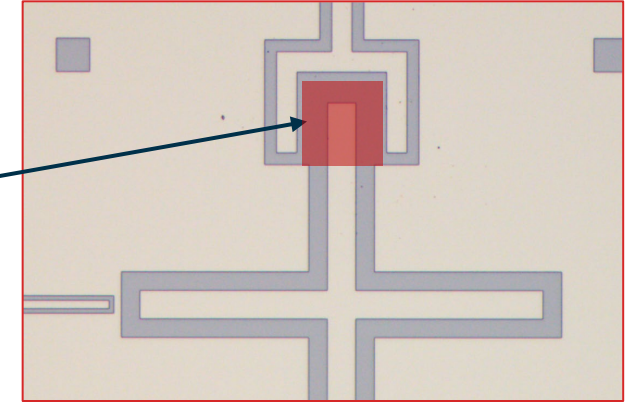
Tunable qubit	Measured	LOM
$\omega_{0 \rightarrow 1} / 2\pi$ [GHz]	5.649	5.649
$L_J$ [nH]	8.364	7.9
$g$ [MHz]	98	100



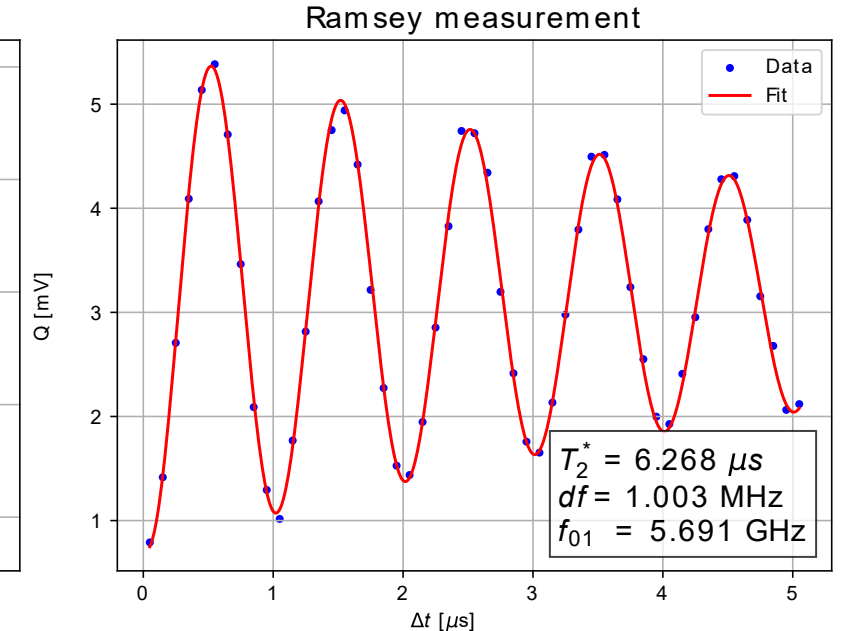
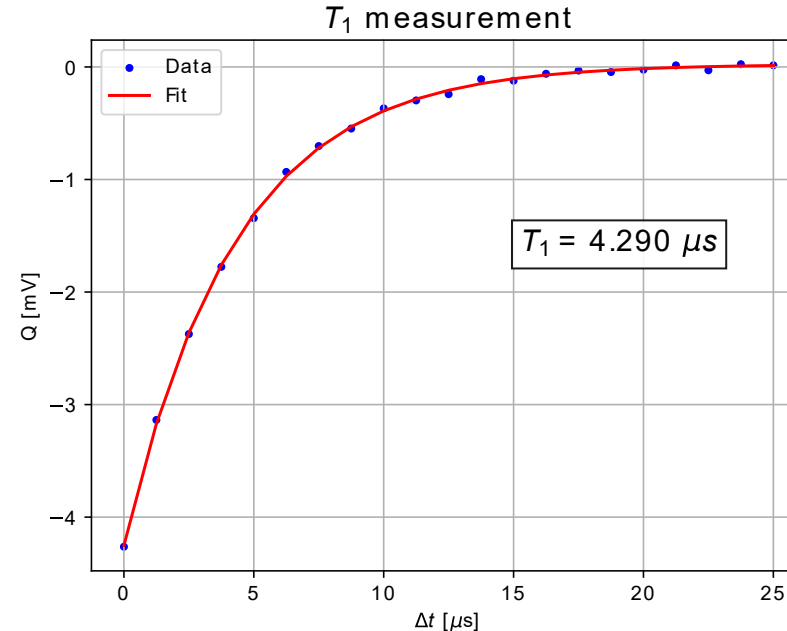
# Chip characterization

$T_1$  and  $T_2$  are **lower than expected** for both qubits.  
This can be due to:

- Possible fabrication issues.
- Qubit frequencies higher than expected.
- No ground between qubit and coupler.
- Insufficient modeling of **Two-Level System (TLS)** losses.



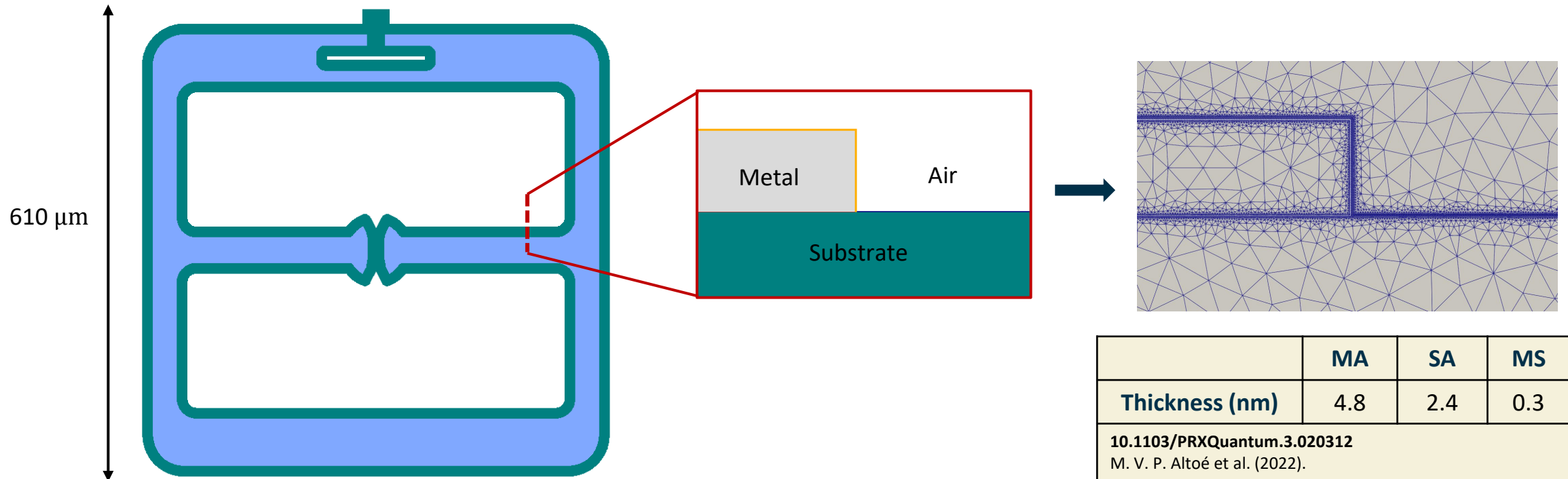
$$\frac{1}{T_{1\text{TLS}}} = \frac{\omega}{Q} = \omega \sum p_i \tan(\delta_i)$$



# Hybrid interface modeling

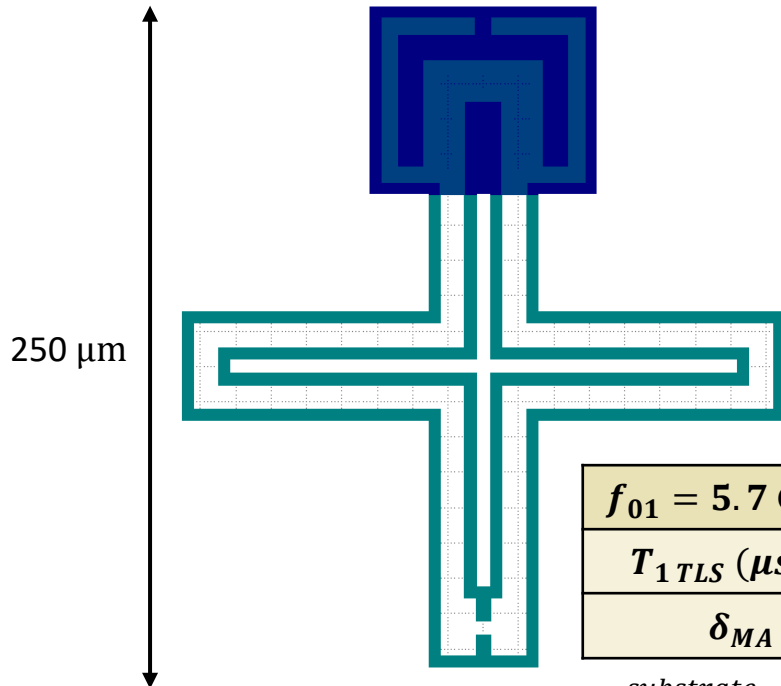
Leverage cross-section (2D) simulations on metal-edge regions (MER) to model surface losses.

- Achieve high-density meshing between interfaces, where the electric field is more intense.
- Computing EPRs on all surfaces, vacuum and substrate.
- Using 2D results to correct for Ansys Eigenmode EPR on customized-regions.
- Engineering shapes to reduce **surface** EPR.



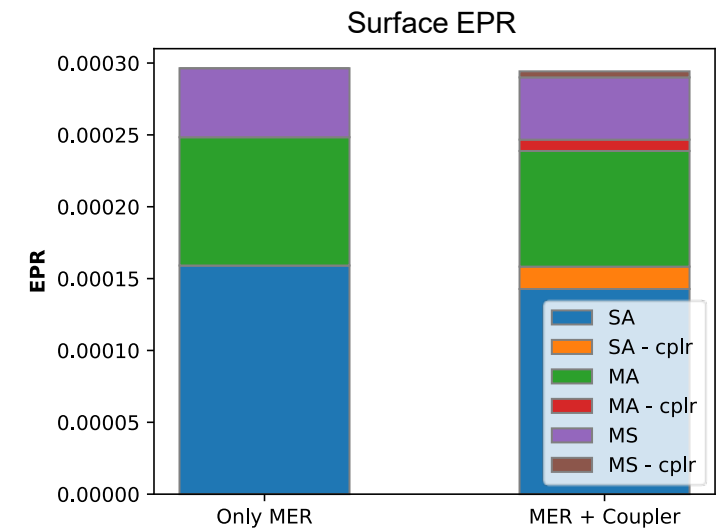
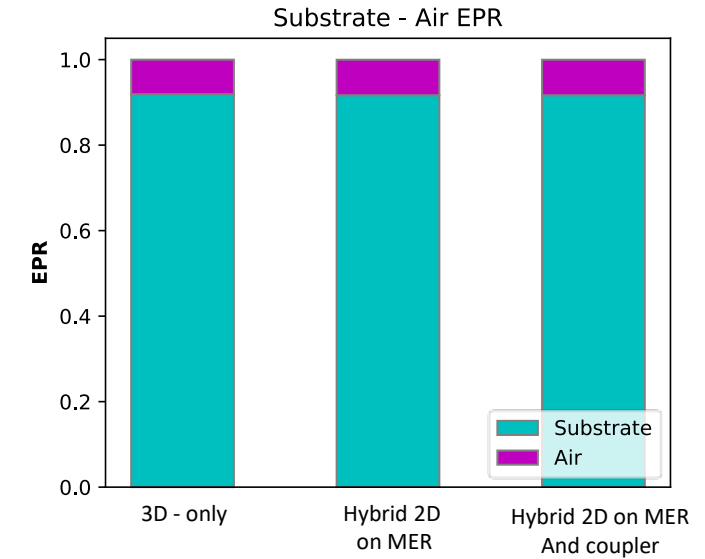
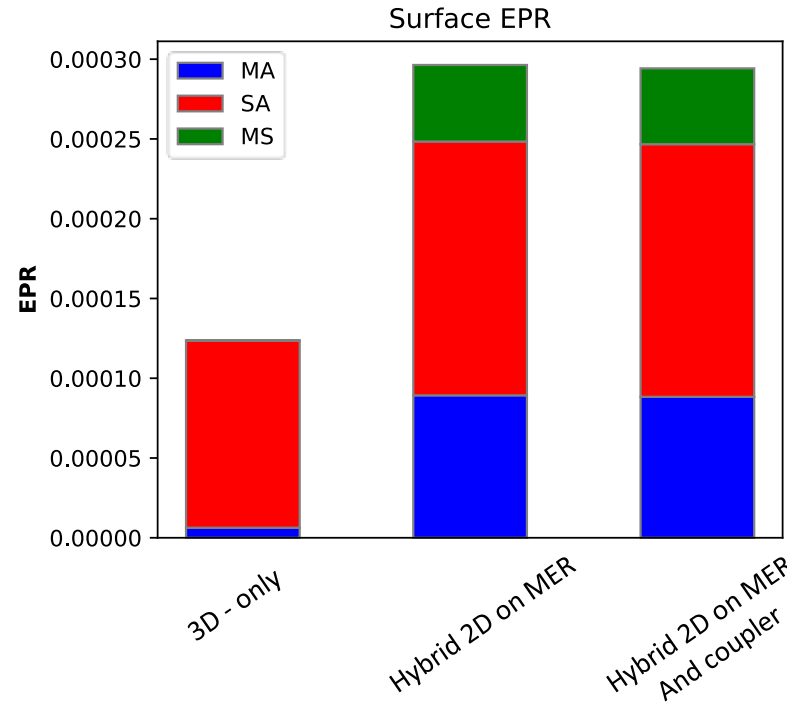
# Improving dielectric loss estimation

- We can select arbitrary regions of interest (MER, couplers, junctions, ...) to carry out 2D simulations and correct the EPR.
- The 3D-only simulation does not capture surface EPR well enough.
- 44% decrease in  $T_{1\,TLS}$  according to hybrid method.



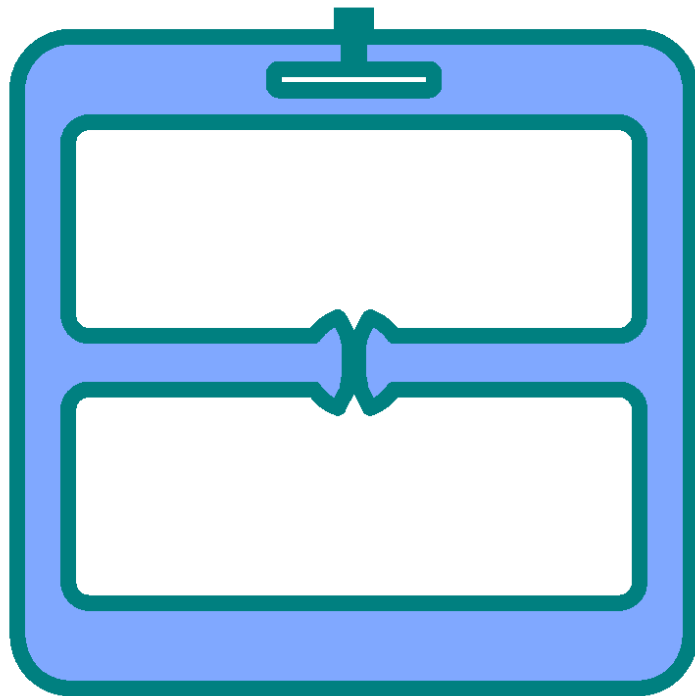
$f_{01} = 5.7\text{ GHz}$	3D - only	Hybrid (MER)	Hybrd (MER + cplr)
$T_{1\,TLS} (\mu s)$	25.9	14.4	14.5
$\delta_{MA} = \delta_{SA} = \delta_{MS} = 5 \times 10^{-3}$ $\delta_{substrate} = 5 \times 10^{-7}$			

$$T_{1\,TLS}^{substrate} = 61\ \mu s$$

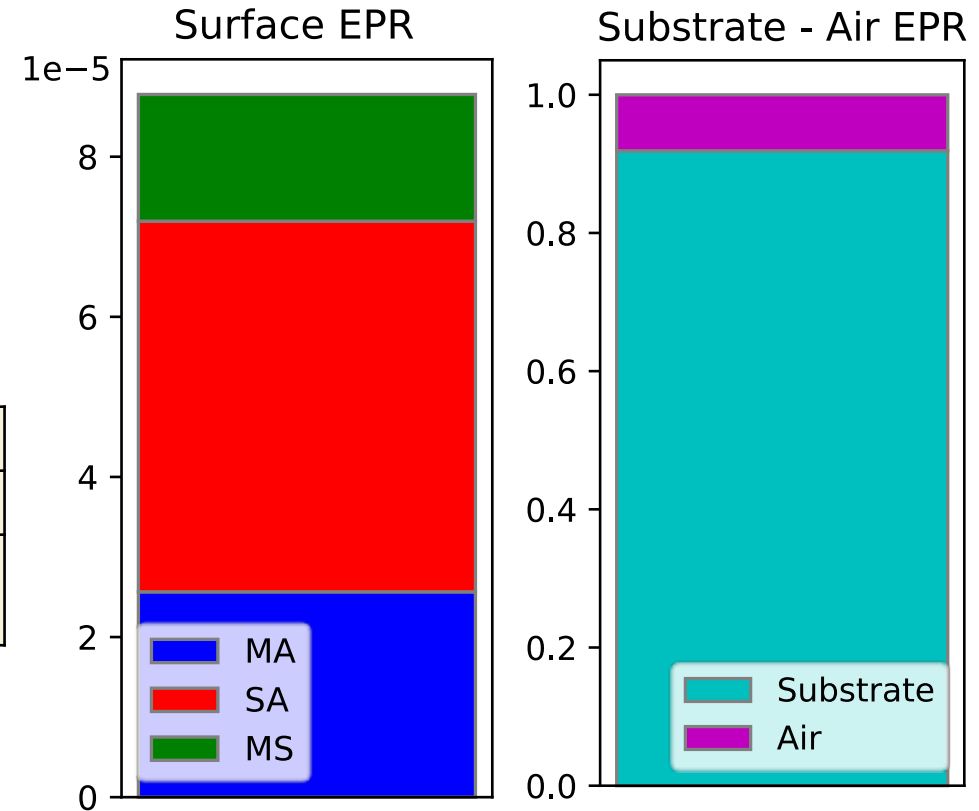


# Double-pad transmon surface loss

- Similar strategy has been carried out for double-pad.
- Bigger area and larger gaps lead to higher coherence time.
- Surface loss decreases by a factor of 3.5.

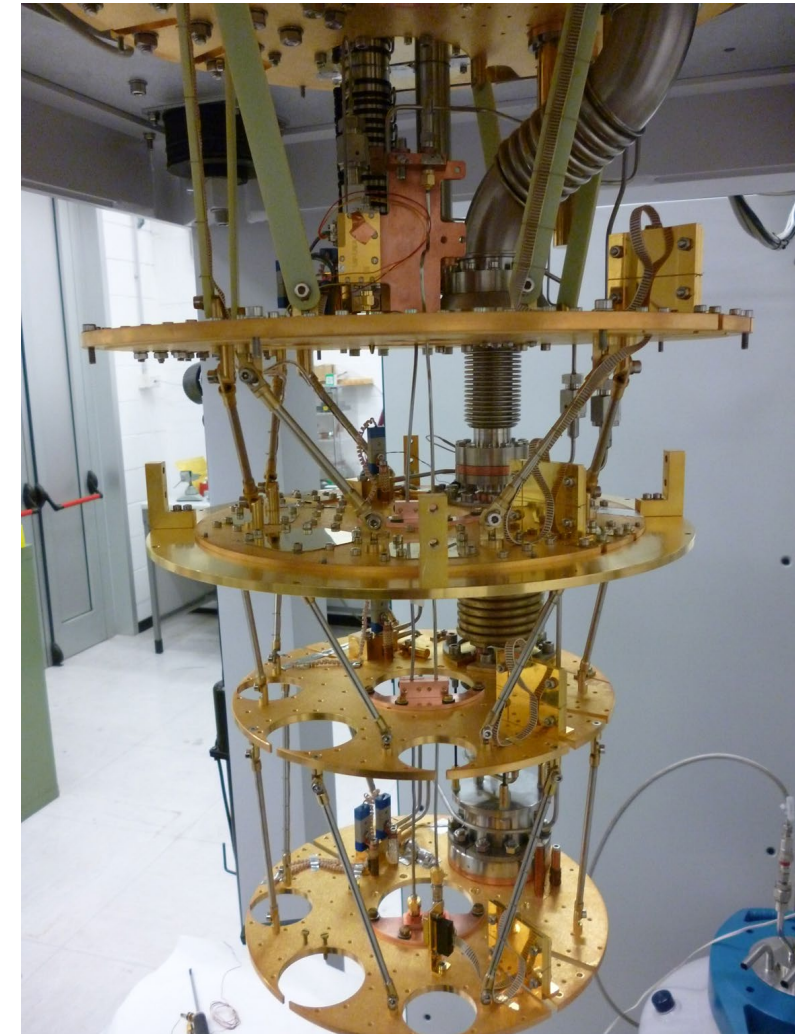


$f_{01} = 5.7 \text{ GHz}$	Hybrid (MER)
$T_{1 TLS} (\mu\text{s})$	31.1
$\delta_{MA} = \delta_{SA} = \delta_{MS} = 5 \times 10^{-3}$ $\delta_{substrate} = 5 \times 10^{-7}$	
$T_{1 TLS}^{substrate} = 61 \mu\text{s}$	



# Future developments

- Modeling and simulation of single-qubit chip has been successfully demonstrated.
- Fabrication and full characterization is being replicated within Qub-IT.
- Other multi-qubit detection schemes are being investigated for QND.
- Further refine the Direct Detection scheme modeling.
- Engineering detection setups.



*Bicocca CryoLab refrigerator*

